

with an aperture half the size of the one above, accepting twice the current, E_{inj} needs to be increased to about 16 Mev.

For beams of particles heavier than the proton, the effect of space charge varies as $(M'/M)^{1/2}$, M and M' being the masses of the proton and the heavier particle, respectively.

In the case of strong-focusing accelerators with com-

paratively small apertures it may be said, in conclusion, that the possibility of radial or axial instability caused by forced resonances places stringent limits on the magnitude of the current that may be stably accepted in any given magnet. This magnitude is independent of the strength of radial and axial focusing and depends only on the radial and axial apertures available and the energy of the particles at injection

The Production of Charged Pions at 180° to the Beam by 340-Mev Protons on Carbon

STANLEY L. LEONARD*

Radiation Laboratory, Department of Physics, University of California, Berkeley, California

(Received October 13, 1953)

The yield of charged pions at $180^\circ \pm 5^\circ$ to the beam produced by 340-Mev protons on carbon has been measured, using nuclear emulsion techniques. Nuclear emulsions embedded in copper, aluminum, or Lucite absorber blocks were exposed to magnetically separated positive and negative pions emitted at 180° by graphite targets bombarded in the electrically deflected proton beam of the Berkeley synchrocyclotron. Plates were exposed for a series of pion energies from 9 to 118 Mev. The developed emulsions were examined with a microscope under high magnification and meson track endings were identified and counted. The values of $d\sigma/d\Omega dT$ as a function of pion energy and the values of $d\sigma/d\Omega$ were calculated for both positive and negative pions. Corrections were made for errors resulting from pion decay in flight, the finite thickness of the target, nuclear interaction of pions in the target and absorber blocks, and background pions. The corrected integrated cross sections are

$$\begin{aligned} d\sigma/d\Omega(\pi^+) &= 1.77 \pm 0.27 \times 10^{-28} \text{ cm}^2/(\text{sterad nucleus}) \quad \text{and} \\ d\sigma/d\Omega(\pi^-) &= 1.90 \pm 0.38 \times 10^{-29} \text{ cm}^2/(\text{sterad nucleus}), \end{aligned}$$

yielding a positive-negative ratio of 9.3 ± 2.3 . An attempt has been made to interpret the positive pion spectrum in terms of existing information on the production of positive pions by protons on hydrogen.

I. INTRODUCTION

A NUMBER of observers have studied the cross sections for production of positive and negative pions when carbon is bombarded by high-energy protons. In particular, the differential cross sections have been measured for pions produced at 0° and 90° to the proton beam, in the laboratory system. These measurements show that the ratio of the differential cross section (integrated over pion energy) for positive pions to that for negative pions at 90° to the beam is either about 5,¹ or about 10,² but that this ratio is much larger at 0° , being about 28.³ The positive pion cross section itself at 0° is either 3 or 6 times as great as at 90° , while the negative cross section is about the same at 0° as at 90° .

In considering these results, it is commonly assumed that the production of pions occurs in the interaction of the incident protons with individual nucleons of the target nucleus. The proton-proton interaction gives rise to positive pions only, by charge conservation, while the

proton-neutron interaction gives rise to pions of both signs. Since the carbon nucleus consists of equal numbers of protons and neutrons, positive pion production would be expected to predominate. If the proton-proton and proton-neutron pion production cross sections inside the nucleus are the same, one would expect the ratio of the total production cross section (integrated over the solid angle) for positive pions to that for negative pions to be about three.

It is, therefore, of interest to measure the production cross sections for pions emerging in the backward direction in order that the total cross sections may be calculated and the positive-negative ratio found for these total cross sections. In addition, such a measurement helps to round out existing information on the production of pions by protons on carbon, and thus on any complex nucleus to the extent that carbon may be considered typical.

II. EXPERIMENTAL METHOD

The technique used in this experiment is essentially the same as that originated by Richman and Wilcox¹ and modified by Cartwright, Richman, Whitehead, and Wilcox⁴ in their measurement of the cross section for

* Now at Principia College, Elsah, Illinois.

¹ Richman, Weissbluth, and Wilcox, *Phys. Rev.* **85**, 161 (1952); C. Richman and H. A. Wilcox, *Phys. Rev.* **78**, 496 (1950).

² Block, Passman, and Havens, *Phys. Rev.* **88**, 1239 (1952); Passman, Block, and Havens, *Phys. Rev.* **88**, 1247 (1952).

³ W. Dudziak (private communication).

⁴ Cartwright, Richman, Whitehead, and Wilcox, *Phys. Rev.* **91**, 677 (1953).

the production of positive pions by protons on protons at 0° . The 340-Mev electrically deflected proton beam of the 184-in. Berkeley synchrocyclotron was used. This beam was collimated in passing through the cyclotron shielding and emerged into the so-called cave area. There (Fig. 1) it passed through an ion chamber and struck a carbon target situated at the farther edge of a region of strong magnetic field.

Pions created in this target and emerging at 180° to the proton beam were deflected by the magnetic field. Those pions in the desired momentum interval passed down channels in brass shielding blocks and struck absorber blocks in which were embedded Ilford C-2 nuclear emulsions. These emulsions were subsequently developed and examined with a microscope under sufficiently high power. The tracks left by negative and positive pions could be recognized, and the number of pion tracks which stopped in the body of the emulsion in a given region was determined. The energy of these mesons was determined by the amount of absorber material they passed through in reaching the region of emulsion scanned. The tables and graphs of the range-energy relation calculated by W. Aron⁵ were used. The number of pions reaching the end of their range and stopping in a given region of the emulsion was a measure of the population density of mesons stopped in that region of the absorber block during bombardment. From the number of meson endings in a given section of the plate, then, the number of pions in the corresponding energy interval emerging from the target at 180° was calculated.

The current from the ion chamber was integrated during the run. Since this instrument had been accurately calibrated by comparison with a Faraday cup, the total number of protons which passed through the target during the bombardment was then known. From these values were calculated the positive and negative pion production cross sections in each energy interval.

The pion detectors in this experiment were, as has been mentioned, nuclear emulsions embedded in blocks of absorber material. The absorber blocks (Fig. 2) were thick enough to stop pions of the energy being investigated. The plates were inclined at an angle of 15° to the horizontal, and, therefore, to the direction of the incoming pions. The angle was chosen somewhat arbitrarily, being small enough that the pions might leave long tracks in the emulsion in order to facilitate identification, and yet larger than 0° so that the mesons might pass directly from absorber to emulsion prior to stopping. This was necessary in order to make it possible to assume that practically the entire path of a pion was in the single medium of the absorber (rather than partly in absorber and partly in the glass backing of the plate), so that the energy could be reliably calculated from the depth in absorber.

⁵ Aron, Hoffman, and Williams, U. S. Atomic Energy Commission Report 663 (unpublished); W. A. Aron, thesis, University of California Radiation Laboratory Report No. 1325 (unpublished).

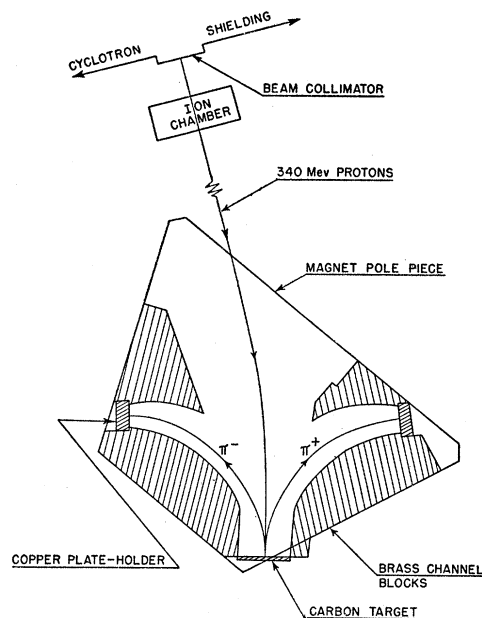


FIG. 1. Schematic diagram of typical experimental arrangement.

The absorber materials were chosen, at the various energies, mainly for convenience. At all high enough energies, copper was used. For the low-energy measurements, it was necessary to use lighter absorber materials (aluminum at 18 Mev and Lucite at 9 Mev) since otherwise the pions in the desired energy interval would have stopped too near the front edge of the emulsion for accurate scanning. Furthermore, the section of the plate corresponding to the desired energy interval would have been so small as to render small uncertainties in its location important. The methods of identification and counting of the tracks of positive and negative pions in the plates under high magnification have been very completely covered elsewhere^{1,4} and will not be further discussed.

In the determination of the number of stopped pions per unit volume of emulsion, it is obviously necessary to know accurately the total volume occupied at the time of exposure by that region of the emulsion which was subsequently scanned. The emulsions are manufactured with a glass backing so that development causes no significant changes in dimensions except in thickness. The surface area of emulsion scanned was measured in conjunction with the scanning operation with the aid of an accurately calibrated microscope stage.

To determine the thickness of the emulsion a series of measurements of the thickness of glass plus emulsion were made on each plate before and after development, using a spring-loaded thickness gauge mounted on a rigid frame with a movable stage. The postdevelopment thickness of the emulsion was measured with the aid of a scale on the fine focus control of the microscope. This scale had been calibrated to ± 2 percent by using it in the measurement of the thickness of a cover glass

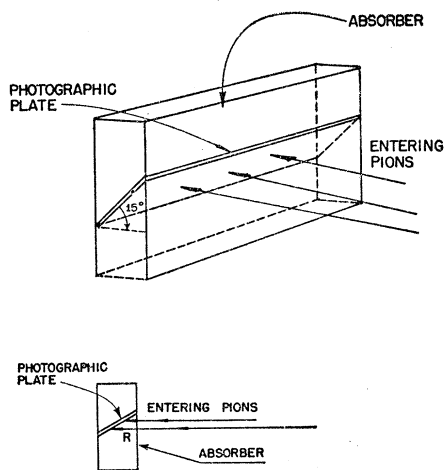


FIG. 2. Absorber block.

whose thickness was accurately known, the indices of refraction of glass, emulsion, and immersion oil being the same to within 1 or 2 percent. From the final thickness and the shrinkage of the thickness at the time of exposure was calculated, the estimated accuracy of the resulting value being ± 3 percent.

The magnetic field used to deflect the pions into the detectors was provided by a large electromagnet originally designed for use as a pair spectrometer. With the pole pieces used in this experiment, the magnet gives a field which is uniform to about 5 percent over a region which extends to within 2 in. of the edges of the pole pieces on all sides. The maximum field which can be maintained over a period of many hours is about 14.3 kilogauss. The gap is 3.4 in.

In the gap between the pole pieces were placed brass channel pieces. These were simply brass shielding blocks with channels cut into them. The channels were designed so that pions in the desired energy interval could emerge from any point of the bombarded area of the target within $\pm 5^\circ$ of 180° and reach any point of the channel exit without striking the channel walls. The brass served to shield the detectors (placed at the channel exits) from stray particles of different momentum, and from pions of the same momentum emitted at angles other than $180^\circ \pm 5^\circ$. The channels thus selected and collimated a rather broad energy interval of pions emitted at 180° into a broad beam of roughly uniform density at the channel exit. In order to obviate the necessity of correcting the results for multiple Coulomb scattering, the direction setup was so arranged that the scanned area of emulsion was effectively in an infinite sea of absorber material during exposure. This was accomplished by seeing that the portions of emulsion scanned were chosen to be at least five times $\sqrt{y^2}$ from either edge of the channel exit during exposure, where $\sqrt{y^2}$ is the rms average lateral dis-

placement from its initial trajectory of a pion of the desired energy at the end of its range in the absorber. As a result of this "bad geometry" arrangement, the number of pions lost from the scanned area by multiple Coulomb scattering in the absorber material was equal, to the first order, to the number of slightly more energetic pions which were scattered into the scanned area. The value of $\sqrt{y^2}$ was calculated for the various absorber materials and pion energies from a formula of L. Eyges⁶ and was of the order of 0.1 cm. The greatest value, at the 118-Mev point, was 0.27 cm.

It is important, of course, to know the solid angle subtended at the target by the scanned volume of emulsion. It can be shown that, in a uniform magnetic field, the solid angle is related to ρ , the radius of curvature of the pion, and to ϕ , the angle through which the pions are turned in passing from the target to the absorber block, by the equation⁷

$$d\Omega/dA = 1/(\rho^2 \phi \sin\phi),$$

where $d\Omega/dA$ is the solid angle per unit projected area perpendicular to the path of the pions.

The error introduced into the calculation of the solid angle by the nonuniformity in the field near the edges of the pole pieces is negligible even though the plate holders were placed at or near the edge of the pole pieces during several of the exposures. The effect of a variation in the radius of curvature caused by this decrease in field strength near the edge is only to shift by a small amount (less than 1°) the angle at which pions of the desired energy must leave the target in order to get down the channel. Since the cross section varies only slowly with laboratory angle (as is seen by comparing the cross sections measured in this experiment with those measured at 90°), a small shift in the angle has a completely negligible effect on the result. The effect of this variation in ρ on the solid angle is likewise negligible, the effective distance of the emulsion from the target being changed by only an infinitesimal amount.

The magnetic field has another possible effect on the result. If the curvature of the pion path in the absorber block is appreciable, the actual length of path of the pion in the absorber may be longer than the apparent value as measured from the front face of the absorber. This difference between actual and measured pion range can be shown to be negligible.⁸ The variation of the field strength with time during any run was less than 1 percent.

III. CROSS-SECTION FORMULA

It can be shown⁴ that the cross section may be expressed in terms of the density of stopped pions by the

⁶ L. Eyges, Phys. Rev. 74, 1534 (1948).

⁷ W. F. Cartwright, thesis, University of California Radiation Laboratory Report No. 1278 (unpublished).

⁸ M. N. Whitehead, thesis, University of California Radiation Laboratory Report No. 1828 (unpublished).

following relation:

$$\frac{d\sigma}{d\Omega dT}(T) = q / \left(\frac{N\rho t}{A} A_0 \frac{d\Omega}{dA} \frac{dT}{dx} \frac{R_{ab}}{R_{em}} \right),$$

where q = density of stopped pions per unit volume of emulsion; N = total number of protons passing through the target; ρt = target thickness in g/cm^2 ; A = atomic weight of target material; A_0 = Avogadro's number; dT/dx = rate of pion energy loss per cm of absorber at energy T ; $d\Omega/dA$ = solid angle per unit projected area perpendicular to the pion path; and $R_{em} = t \csc\alpha$, where t = thickness of emulsion and α is the angle at which the emulsion is inclined to the path of the pions. R_{ab} is the range in the absorber material of a pion whose range in emulsion is R_{em} . The values of R_{ab}/R_{em} are: for copper, 0.414; for aluminum, 1.14; and for Lucite, 2.02.

IV. CORRECTIONS

Because of the smallness of the production cross section at 180° , particularly for negative pions, it was necessary that the proton beam flux be as large as possible. As a result, the collimators used had fairly large diameter (usually two inches) and some protons in the wings of the beam struck the pole pieces of the magnet before reaching the production target. Some pions were produced in the iron of the pole pieces at such energies and angles as to be able to travel down the channels into the detectors. There were thus background pions of both signs in both positive and negative detectors. To correct for this flux of background pions, plates were exposed in the same geometry as the plates used for the cross-section measurement, but with the production target removed. The background plates were developed and scanned with the others, and the contribution from the background flux to the total density of stopped pions was subtracted. At two of the energies, 75 and 118 Mev, it was inconvenient to expose background plates. For the 75-Mev cross sections, the correction was estimated from the measured corrections at the other energies by comparing the numbers of positive pions found in the negative pion plates. At the 118-Mev point no negative plate was exposed, so that the correction had to be estimated from the corrections at other energies on the basis of the total number of pions found. Very little error was introduced in this way, since the background correction is relatively small at all energies. Furthermore, the cross sections themselves are relatively quite small at 75 and 118 Mev, so that uncertainties in the correction are less important than at the lower energies.

In addition, the cross sections were corrected for the following effects:

- (a) Pions emerging from the target at energy T in an interval ΔT were created at different depths of the target in different energy intervals $\delta T'$. Since we measure ΔT , we must correct the calculated

cross section for the difference between ΔT and the various $\delta T'$.

- (b) Some of the pions created in the target decayed in flight before reaching the detector.
- (c) Some of the pions entering the absorber material were absorbed or scattered through large angles by the nuclei in the absorber.

These corrections were made in the manner described by Cartwright *et al.*,⁴ except that in the nuclear interaction correction a total attenuation cross section equal to nuclear area was assumed, independent of pion energy. This last correction is of course not precise, but the available data on the cross section for pion absorption and large-angle scattering are still insufficient to make the correction more accurate. Fortunately, this correction is important mainly at the higher energies where the pion production cross sections are so small that the uncertainty in the correction is not serious. Even though the percentage uncertainty is rather large, the absolute uncertainty is quite small.

V. RESULTS

The measured cross sections are given in Tables I and II, along with the various correction factors; for target thickness, k_{th} ; for pion decay in flight, k_{dec} ; and for nuclear interaction, k_{nuo} .

The errors given are probable errors of purely statistical origin. In addition, the results are subject to a number of systematic errors. Among these are the scanning efficiency of the observer, inaccuracies in the ion chamber calibration, uncertainties in the stopping power of emulsion, and uncertainties in the emulsion thickness measurements. The energy width shown for each of the points is the larger of the widths ΔT and δT , where ΔT is the energy interval determined by the width of the region scanned in the emulsion, and δT is the energy width of the target.

The calculated values of $d\sigma/d\Omega dT$ are plotted *versus* T in Figs. 3 and 4. The curves drawn through the points are merely smooth curves fitted by eye and have no theoretical significance. The integrated cross sections have been obtained by integrating the area under these curves, as corrected for nuclear interaction. The systematic errors mentioned above are estimated to give a net uncertainty of ± 10 percent to the results. Because of these errors, as well as the lack of precision of the nuclear interaction correction, an error of ± 15 percent is assigned to the value of $d\sigma/d\Omega$ for positive pions, and an error of ± 20 percent of the value of $d\sigma/d\Omega$ for negative pions. These values are intended to include the statistical errors and should be considered probable errors. The results for the differential cross sections integrated over pion energy are

$$d\sigma/d\Omega(\pi^+) = 1.77 \pm 0.27 \times 10^{-28} \text{ cm}^2/(\text{sterad nucleus}),$$

$$d\sigma/d\Omega(\pi^-) = 1.90 \pm 0.38 \times 10^{-29} \text{ cm}^2/(\text{sterad nucleus}).$$

TABLE I. Positive pion cross sections.

T	$\left(\frac{d\sigma}{d\Omega dT}\right)_{\text{uncorr}}$		K_{th}	K_{dec}	$\left(\frac{d\sigma}{d\Omega dT}\right)_{\text{corr}^a}$	K_{nuc}	$\left(\frac{d\sigma}{d\Omega dT}\right)_{\text{corr}}$
9.2±1.2 Mev	2.01 ±0.18×10 ⁻³⁰	cm ²	1.10	1.091	2.41±0.21×10 ⁻³⁰	1.008	2.43 ±0.21×10 ⁻³⁰
17.8±2.8	2.83 ±0.21	sterad Mev nucleus	1.16	1.122	3.68±0.28	1.026	3.78 ±0.29
31.9±1.9	2.60 ±0.18		1.04	1.095	2.97±0.20	1.064	3.16 ±0.21
51.5±1.5	1.33 ±0.11		1.00	1.073	1.42±0.12	1.143	1.62 ±0.14
75 ±5.0	0.56 ±0.05		1.00	1.074	0.60±0.05	1.278	0.77 ±0.06
118.6±8.6	0.056±0.014		1.00	1.072	0.06±0.015	1.627	0.097±0.024

^a Corrected for everything except nuclear interaction.

The positive-negative ratio at 180° is thus equal to 9.3±2.3. These results are based on a total of 570 pion-muon decay events and 136 negative pion stars.

Using the values of $d\sigma/d\Omega$ measured in this experiment along with those for pions emerging at 0° and 90° to the beam, one can integrate roughly over the entire solid angle to obtain the total cross sections. The results are approximately $\sigma(\pi^-) = 5.7 \times 10^{-28}$ cm² and $\sigma(\pi^+) = 47.6 \times 10^{-28}$ cm², giving a positive-negative ratio of 8.4. Since this is much larger than three, it is clear that the proton-proton and proton-neutron pion production cross sections inside the carbon nucleus are not the same.

The salient differences in the spectra for positive and negative pions (Figs. 3 and 4) are the differences in the location of the peak and in the location of the high-energy cutoff. It is seen that the negative spectrum peaks at a lower pion energy and has a high-energy cutoff at a lower pion energy than is the case for positive pions. These features, which are also found in the positive and negative spectra at 0° and 90°, can be understood tentatively in terms of a nucleon-nucleon picture of the production process. Energetic pions could not be produced at 180° to the beam if it were not for the fact that the individual nucleons in the carbon nucleus have fairly large internal momenta. It then appears that the creation process for positive pions may have a steeper excitation function than that for negative pions, so that the positive pion process takes greater advantage of the higher momentum components of the nucleons in carbon. The large positive-negative production ratio may also be understood in terms of this picture. Thus, there seems to be a fundamental difference between the primary production processes for

positive and negative pions. This may perhaps be explained in terms of a difference between the $p-n$ interaction and the $p-p$ interaction. One may imagine that the $p-p$ interaction can result in a closely associated pair of nucleons, in analogy to the free nucleon reaction $p+p = \pi^+ + d$. An attempt to analyze the positive spectrum in terms of such a picture is described in the next section.

VI. ANALYSIS OF POSITIVE PION SPECTRUM ON NUCLEON-NUCLEON MODEL

An attempt has been made to interpret the positive pion spectrum measured in this experiment in terms of pion production in nucleon-nucleon collisions. Similar analyses have been carried out by Henley⁹ for positive pion production at 0° and 90° by protons on carbon, by Passman, Block, and Havens² in the case of positive pion production at 90° by protons on various nuclei, and also by Neher¹⁰ in the case of positive and negative pion production at 90° by neutrons on carbon.

If one assumes that negative pion production in proton-neutron collisions is roughly as probable as is the production of positive pions in the same type of collision, then it is clear that most of the positive pions produced by proton bombardment of carbon must result from proton-proton collisions. This is to be inferred from the fact that the positive-negative ratio has been found to be about 9 and the additional fact that negative pions in this experiment can only result from $p-n$ collisions. It has therefore been assumed in this analysis that only $p-p$ collisions are involved in the production of positive pions from carbon.

It has also been assumed that in each pion-producing collision the resulting nucleons leave in such a way

TABLE II. Negative pion cross sections.

T	$\left(\frac{d\sigma}{d\Omega dT}\right)_{\text{uncorr}}$		K_{th}	K_{dec}	$\left(\frac{d\sigma}{d\Omega dT}\right)_{\text{corr}^a}$	K_{nuc}	$\left(\frac{d\sigma}{d\Omega dT}\right)_{\text{corr}}$
9.6±1.6 Mev	3.67±0.60×10 ⁻³¹	cm ²	1.10	1.091	4.41±0.72×10 ⁻³¹	1.008	4.47±0.73×10 ⁻³¹
17.8±2.8	2.64±0.43	sterad Mev nucleus	1.16	1.122	3.44±0.56	1.026	3.53±0.57
31.9±1.9	2.63±0.30		1.04	1.095	3.00±0.34	1.064	3.19±0.36
51.5±1.5	1.66±0.28		1.00	1.073	1.78±0.30	1.143	2.03±0.34
75 ±5.0	0.30±0.08		1.00	1.074	0.32±0.09	1.278	0.41±0.12

^a Corrected for everything except nuclear interaction.

⁹ E. Henley, Phys. Rev. **85**, 204 (1952).

¹⁰ L. Neher, thesis, University of California Radiation Laboratory Report No. 2191 (unpublished).

that the pion gets the maximum possible kinetic energy—that is, that the resulting nucleons form a deuteron. This has been assumed for several reasons. First, it is known that in the bombardment of free protons by protons, the deuteron-forming reaction produces ~ 70 percent of the positive pions.⁴ In addition, the analysis of Passman, Block, and Havens, which gives a reasonably good fit to the experimental data on pion production from carbon at 90° , is based on the same assumption. Further still, the analysis of Henley involves the assumption that the deuteron-producing reaction does not contribute appreciably, and that analysis fails to account for the positive pion spectrum from carbon at 0° or for the positive-negative ratio at that angle. Moreover, a compelling reason for making this assumption is that it results in a considerable simplification of the calculations.

Such an analysis as this involves knowledge of the momentum distribution of the nucleons in the carbon nucleus and of the energy dependence of the nucleon-nucleon pion production cross section. This calculation has been carried out for two types of momentum distributions, the Chew-Goldberger distribution,¹¹ and a Gaussian distribution with a width corresponding to 16 Mev. This last distribution was chosen because Cladis, Hess, and Moyer¹² have found that Gaussians of widths ranging from 14 to 19 Mev can be used to fit their measured values for the cross sections at various angles for quasi-elastic scattering of protons in carbon. Two different excitation functions were also used, with energy dependences of T'^2 and T'^3 , where T' is the maximum energy of the pion resulting from the nucleon-nucleon interaction, expressed in the center-of-mass system of the two interacting nucleons. These excitation functions were adjusted for approximate fit to the experimental points for production at 0° from free protons as measured by Schulz¹³ and calculated by him from the data of Durbin, Loar, and Steinberger¹⁴ on the inverse reaction. The energy-dependence values were chosen for the following reasons: the T'^2 dependence because Passman, Block, and Havens² found that it gave best agreement with their experimental data, the T'^3 dependence because it is the steepest energy dependence which has any relation to the phenomenological matrix elements obtained by Passman *et al.*, in extending the treatment of Watson and Brueckner.¹⁵

In addition to variations in excitation functions and momentum distributions, the analysis has been carried out for two different models of the kinematic situation. One can assume that the incoming nucleon selects one of the nucleons of the carbon nucleus, and interacts with it, with the resulting pion emerging so rapidly

¹¹ G. F. Chew and M. L. Goldberger, *Phys. Rev.* **77**, 470 (1950).

¹² Cladis, Hess, and Moyer, *Phys. Rev.* **87**, 425 (1952); P. Wolff, *Phys. Rev.* **87**, 434 (1952).

¹³ A. G. Schulz, Jr., thesis, University of California Radiation Laboratory Report No. 1756 (unpublished).

¹⁴ Durbin, Loar, and Steinberger, *Phys. Rev.* **84**, 581 (1951).

¹⁵ K. Watson and K. Brueckner, *Phys. Rev.* **83**, 1 (1951).

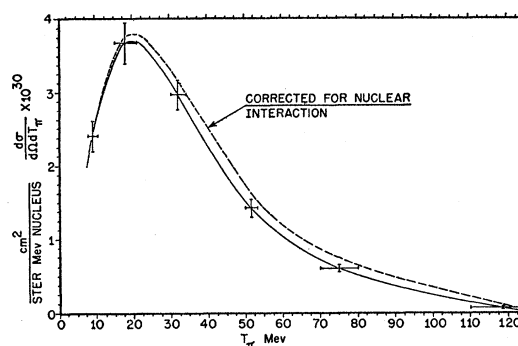


FIG. 3. Plot of differential cross section for production of positive pions as a function of energy. The solid curve has not been corrected for nuclear interaction. The dashed curve has been so corrected.

that the reaction is over, as far as the pion is concerned, before the rest of the nucleus can react in any way. In this "impulse-approximation" model, the calculation is carried out as if the nucleus consists merely of a set of particles whose relationship to each other has the sole effect of imparting to each a momentum relative to the others. When energy and momentum are balanced, only the two interacting nucleons are considered. This model, of course, overestimates the energy available to produce pions, since in reality the rest of the nucleus does absorb some energy and momentum, as is shown by the experiment of Ford¹⁶ on the production of pions by neutrons on oxygen in a cloud chamber. In addition, the momentum distribution gives a finite probability that the struck nucleon has sufficient internal momentum to permit the production of a pion whose kinetic energy is so large as to violate over-all energy conservation. In the case of production at 180° , however, the pion energies considered are all well below the limiting value determined by over-all energy conservation.

The other model for the kinematics used in this analysis is essentially that used by Neher¹⁰ and involves

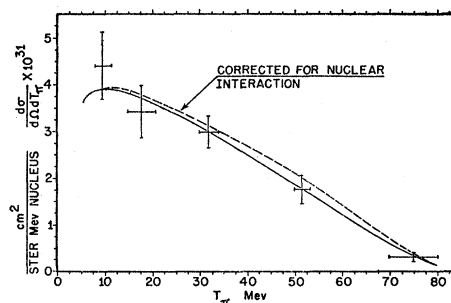


FIG. 4. Plot of differential cross section for production of negative pions as a function of energy. The solid curve has not been corrected for nuclear interaction. The dashed curve has been so corrected.

¹⁶ F. C. Ford, thesis, University of California Radiation Laboratory Report No. 2148 (unpublished); F. C. Ford (private communication).

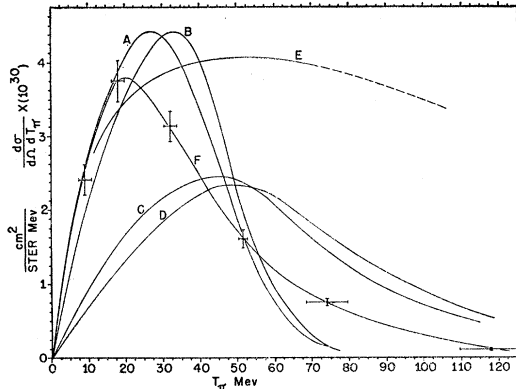


FIG. 5. Experimental spectrum of positive pions with theoretical spectra calculated on a nucleon-nucleon model and normalized to the area of the experimental curve.

considering the rest of the nucleus in the energy and momentum balance. The incoming nucleon is assumed, as before, to select for interaction one of the nucleons of the target nucleus. If this struck nucleon has a momentum p , then the rest of the nucleus must be recoiling with momentum $-p$. After the collision, the residual nucleus, with changed mass, carries off kinetic energy and momentum, as do the pion and deuteron. The selection of an appropriate average value for the new mass of the residual nucleus involves an estimate of its average excitation. The new mass M' was set equal to $M - m + \epsilon/c^2$, where M is the mass of the C^{12} nucleus, m is the proton mass, and ϵ is 20 Mev. The value of 20 Mev was chosen to include 8-Mev binding energy for the removed proton (carried off in the deuteron), plus about 12-Mev excitation for the residual nucleus, a figure arrived at from a consideration of the data of Ford.¹⁶

These calculated spectra were corrected for the attenuation of the incident protons and the reabsorption of the pions in nuclear matter.

The theoretical spectra resulting from this analysis are shown in Fig. 5. All curves are normalized to have the correct experimental area, $d\sigma/d\Omega$. Curves *A*, *B*, *C*, and *D* were all calculated using a Gaussian momentum distribution, the first two on the Neher model of the kinematics and the latter two on the impulse-approximation model. Curves *A* and *C* were calculated using a $T^{3/2}$ excitation function, while curves *B* and *D* involved use of a $T^{1/2}$ energy dependence. Curve *E* is intended to show the general result of using a Chew-

Goldberger momentum distribution with either of the kinematic models and either of the excitation functions. The exact values for the cross sections could not be calculated in the case of the Chew-Goldberger distribution without much additional work. However, the analysis was carried far enough to show that the result is in general the deplorable one shown in the diagram. Curve *F* is the experimentally measured spectrum. It must be remarked that the area under the curves before normalization differed widely. Curves *A*, *B*, *C*, and *D* had to be multiplied by factors of 31.3, 17.4, 9.3, and 4.1, respectively, to normalize them.

It is seen that the Neher model gives a better fit to the experimental spectrum shape than does the impulse approximation, but that only the impulse approximation with a $T^{1/2}$ excitation gives anything like the experimental value of the integrated area before normalization. It is clear, then, that none of the variations makes possible a really adequate interpretation of the carbon spectrum in terms of the proton-proton spectrum. Even use of the Chew-Goldberger momentum distribution was found not to change the values of $d\sigma/d\Omega dT$ in the region of interest (at the few values of the pion energy for which the exact value could be obtained) by a factor of more than about 1.2, though the values of $d\sigma/d\Omega dT$ at higher energies are changed considerably, in a direction in disagreement with the experimental results.

It is difficult to see how any variation in kinematic model or momentum distribution could bring the calculated spectrum into reasonable agreement with the observed one. It is believed to be possible (on the basis of several attempts in this direction) to pick an arbitrary excitation function such that a good fit could be obtained, but such a function would be so steep (proportional to T^n , where $n \geq 8$) and so arbitrary in shape as to be meaningless.

VII. ACKNOWLEDGMENTS

This experiment was first suggested by Professor C. Richman, whose constant encouragement and advice throughout the course of the work have been greatly appreciated.

I would like to thank Dr. S. Bludman for many stimulating discussions about the theoretical aspects of the paper.

The assistance of Miss I. D'Arche and Mrs. B. Baldridge in scanning some of the plates is gratefully acknowledged.